Modeling of Source/Drain Access Resistances and their Temperature Dependence in GaN HEMTs

Sudip Ghosh, Sheikh Aamir Ahsan,
and Yogesh Singh Chauhan
Nanolab, Dept. of Electrical Engineering,
Indian Institute of Technology Kanpur, India
Email: sudip@iitk.ac.in

Sourabh Khandelwal
Dept. of Electrical Engineering and Computer Science,
University of California Berkeley, USA

***Abstract*—In this paper, we present the modeling of source/drain access resistances in the surface potential based model named "Advanced Spice Model for High Electron Mobility Transistor" (ASM-HEMT) for AlGaN/GaN HEMTs. From TCAD simulation, it is shown that nonlinear source and drain resistances increase with drain current which is due to the saturation of electron velocity in this region. Accurate modeling of this access resistance is of immense importance to correctly predict the drain current, transconductance (g_m) and hence the transit frequency (f_T) at higher current. The model shows excellent agreement with experimental data at room temperature. Variation of measured ON-resistance (R_{ON}) with temperature is well predicted by model which justifies the accuracy of temperature dependence model of source/drain resistances.**

***Index Terms*—Source/drain resistance, access region, temperature dependence, AlGaN/GaN HEMTs.**

I. Introduction

AlGaN/GaN High Electron Mobility Transistor (HEMT) has emerged as a promising candidate for high frequency, high power as well as high temperature applications [1], [2]. GaN based HEMT is able to simultaneously offer high breakdown voltage and wide bandwidth due to the interesting features of III-nitride system, such as wide bandgap, large 2-DEG charge density, high electron mobility and improved thermal conductivity with SiC substrates [3]. Aggressive lateral scaling of source-drain access regions improve the RF performance of GaN HEMT but at the cost of breakdown voltage (BV). Too short gate to drain distance (L_{gd}) increases electric field which is responsible for lowering of BV. Scaling of L_{gd} also affects the f_{max} due to increasing C_{gd} and output-conductance (g_{ds}) of device. As a trade-off, a short gate to source distance L_{gs} and optimized L_{gd} is required to achieve high f_T, f_{max} and BV altogether [4]. For very high power device gate field-plate structure [2] is often used to increase BV by redistributing the electric field and reducing its peak value at the gate edge of drain side. In GaN HEMT, gate-to-drain/source access region works as nonlinear resistance ($R_{d/s}$) which limits maximum drain current. Accurate model of $R_{d/s}$ is of great importance to predict the drain current and transconductance for high power as well as high frequency GaN HEMTs [5].

In this paper, we implement drain current dependent $R_{d/s}$ model in a surface potential based compact model named ASM-HEMT [6–11], which is under standardization at the Compact Model Coalition (CMC) [12]. The intrinsic drain current is obtained [8] using drift-diffusion framework using surface potential (ψ) expression which in turn is evaluated from an improved analytical calculation of quasi-Fermi potential E_F, considering the two important energy levels within the triangular potential well, valid in all regions of device operation.

II. Source and Drain Access Resistance Model

The drain/source resistance consists of bias independent contact resistance (R_c) and access region resistance $R_{d/s}$, which depends on the amount of current flowing through this region. The current flowing through the access region can be defined as $I_{acc} = W \cdot NF \cdot q \cdot n_{s0} \cdot v_s = Q_{acc} \cdot v_s$, where W is the gate width, NF is the number of finger, q is the electron charge, n_{s0} is the fixed 2-DEG charge density in the drain or source side access region and v_s is the electron velocity. As n_{s0} does not change significantly with increasing V_d, to support the increasing currents, v_s should increase. Initially v_s increases linearly but, then it saturates to saturation carrier velocity v_{sat}, with the voltage drop V_R across the access region. The current flowing through access region can be expressed as [5], [13], [14]:

$$I_{acc} = Q_{acc} \cdot v_s = Q_{acc} \cdot \frac{v_{sat} \cdot V_R}{[V_{Rsat}^{\gamma} + V_R^{\gamma}]^{\frac{1}{\gamma}}} \tag{1}$$

where $V_{Rsat} = L_{acc} \cdot v_{sat}/\mu_{acc}$, is saturation voltage of access region, L_{acc} is the length of source/drain side access region, μ_{acc} is the carrier mobility and γ is a smoothing parameter. Now $R_{d/s}$ can be expressed in terms of drain current I_d through the formulation:

$$R_{d/s} = \frac{V_R}{I_{acc}} = \frac{R_{d0/s0}}{\left[1 - \left(\frac{I_d}{I_{acc,sat}}\right)^{\gamma}\right]^{\frac{1}{\gamma}}} \tag{2}$$

where $I_{acc,sat} = Q_{acc} \cdot v_{sat}$, is the saturation current or maximum current supported in the access region and low current access resistance $R_{d0/s0} = L_{acc}/(Q_{acc} \cdot \mu_{acc})$. From (2), we can observe that $R_{d/s}$ increases rapidly as I_d approaches to $I_{acc,sat}$ which limits the total drain current flowing through the device.

978-1-5090-1830-7/16/$31.00

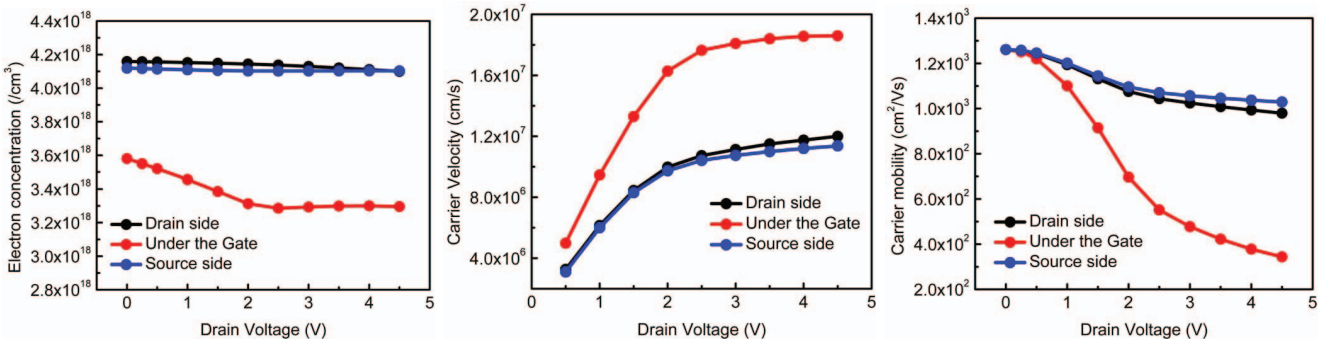

(a) (b) (c)

Fig. 1: Variation of (a) carrier charge density, (b) electron velocity and (c) electron mobility with V_d probed at source side, drain side access region and under the gate channel region.

III. Temperature Dependence of Access Resistance

The temperature dependence of $R_{d/s}$ model is extremely important as it increases significantly with increasing temperature especially for the short channel devices. The temperature dependence of 2-DEG charge density in the drain or source side access region is given by:

$$n_{s0}(T) = NS0ACC \cdot \left(1 - KNS0 \cdot \left(\frac{T}{TNOM} - 1\right)\right) \quad (3)$$

where $NS0ACC$ is a parameter extracted at $TNOM$ and $KNSO$ is the temperature dependence parameter. At the time of implementation, we restrict the value of the total multiplication factor of $NS0ACC$, using hyperbolic smoothing to avoid the negative value of $n_{s0}(T)$ at a sufficiently high temperature.

The carrier velocity in the 2-DEG layer slowly varies with temperature [15]. With increasing temperature, scattering is increased due to the enhanced lattice vibration, resulting in reduction of electron velocity. The temperature dependence of saturation velocity can be modeled as a linear function as follows [16]:

$$V_{sat}(T) = VSATACCS \cdot [1 + ATS(T - TNOM)] \quad (4)$$

where $VSATACCS$ is the saturation velocity extracted at $TNOM$ and ATS is the model parameter. Similar smoothing is also needed for the high temperature case where $V_{sat}(T)$ can go to negative as ATS is negative.

Phonon scattering, surface scattering and coulomb scattering (including ionized impurity and interface charge scattering) are the three major scattering mechanisms which affect the electron mobility in the 2-DEG layer of AlGaN/GaN HEMT. Polar optical phonon scattering becomes the dominant mechanism [17] at higher temperature. The temperature dependence of electron mobility in access region is modeled following a power law, which is consistent with optical phonon scattering limited mobility [18] and is given by:

$$\mu_{acc}(T) = U0ACC \cdot \left(\frac{T}{TNOM}\right)^{UTEACC} \quad (5)$$

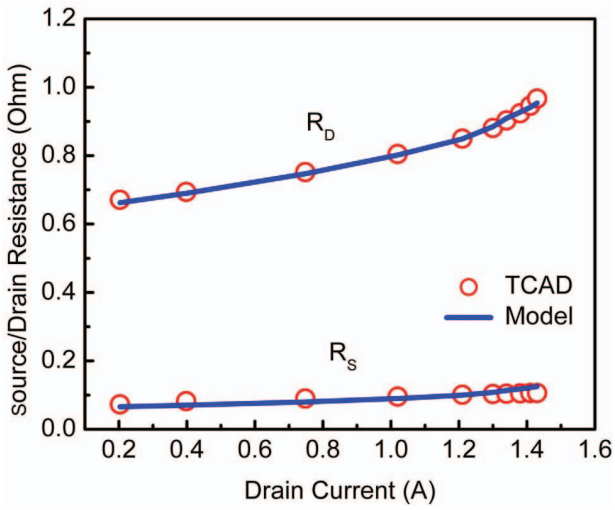

Fig. 2: Nonlinear variation of source/drain access resistances with drain current extracted from TCAD simulation and comparison with model.

where $U0ACC$ is the low field mobility parameter for access region at room temperature and $UTEACC$ is the power parameter which describes the temperature dependence.

IV. TCAD Validation of $R_{d/s}$ Model

To verify the theory of access resistance model, we have performed TCAD simulation (Silvaco ATLAS) on a AlGaN/GaN HEMT structure (L_g=0.125 µm, W=900 µm, L_{sg}=0.2 µm, L_{dg}=1.7 µm, AlGaN layer thickness 20 nm). In the device structure, we choose three different points on the 2-DEG confinement; at source side access region; under the gate and at drain side access region. Carrier sheet charge density, electron velocity and mobility are probed on those three points with varying V_d and fixed V_g. From Fig. 1(a), we can observe that the electron charge density is almost constant in the access region whereas under the gate its quantity is low and decreases with increasing V_d. Under the gate metal, a strong electric field acts across the AlGaN barrier layer which in turn push the 2-DEG electrons away from the gate, resulting in reduction of charge density in the channel compared to

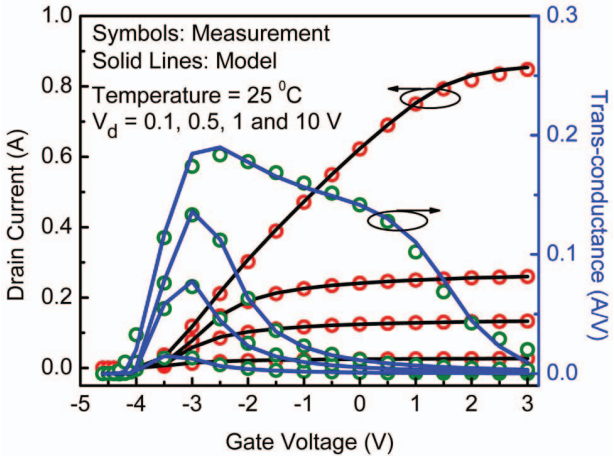

Fig. 3: Accurate fitting of $I_d - V_g$ (left-Y axis), and trans-conductance (right-Y axis) plots at 25°C for the toshiba power GaN HEMT device data (L_g=1 µm, W=3 mm, L_{sg}=2 µm, L_{dg}=14 µm, AlGaN layer thickness 30 nm)(symbol and solid line signifies the measurement and model); in the g_m-V_g plot, for higher V_d (10V), different slopes are observed above threshold-voltage; self-heating effect (thermal resistance parameter) can accurately predict the first slope and the second slope is mainly governed by the velocity saturation parameter of the access region resistance model; curves for low V_d almost saturates after a certain V_g due to the high access region resistance.

the access region. To support same current, charge velocity product should be constant throughout the channel and access region which implies higher carrier velocity under the gate compared to access region shown in Fig. 1(b). The saturation of carrier velocity after a certain V_d, which is less in the access region mainly limits the drain current flowing through the device. The mobility variation with V_d is presented in Fig. 1(c) which follows the velocity saturation model. We extract the source and drain access region resistances and plot with I_d (Fig. 2), clearly support the $R_{d/s}$ model. Initially, source and drain resistances increase slowly and as I_d approaches to its higher value, the resistance starts to increase rapidly setting the limit of maximum drain current which can flow through the 2-DEG layer. Excellent agreement between source and drain access resistances variation with drain current between the TCAD extracted data and model (extracted through the fitting of $I_d - V_d$ and $I_d - V_g$ characteristics) strongly justifies the accuracy of the model formulation.

V. Results and Discussions

To validate our drain current dependent $R_{d/s}$ model, we show fitting results with measured data for power GaN HEMT device. The data is provided from Toshiba as a part of Si2-CMC model standardization activity. The parameter extraction is performed using Keysight ICCAP software. The channel length and width of the device are 1 µm and 3 mm respectively, with gate-to-source and gate-to-drain distance 2 µm and 14 µm, respectively. This GaN HEMT device has metal-insulator-semiconductor (MIS) structure with AlGaN thickness of 30 nm. The I-V characteristics are measured with curve tracer in pulsed mode where pulse width and period used are 2 ms and 100 ms respectively.

The model parameters for room temperature data have been extracted using the standard parameter extraction procedure for the ASM-HEMT model and the good agreement with measured data is shown in Fig. 3 and Fig. 4. The $I_d - V_g$ and $g_m - V_g$ presented in Fig. 3 (left and right Y-axis respectively) show that at higher gate voltage, the access region resistance dominates and current flattens out with increase in V_g. From the trans-conductance (g_m) plot, different slopes in the linear-to-saturation transition region and in the saturation region are observed for the higher V_d (=10V) curve. The first slope degradation in g_m at medium V_g is mainly due to the self-heating effect, whereas the second slope is dominated by the velocity saturation effect in the non-linear access region resistance model. Although the measurements have been performed in pulsed mode, the self-heating effect is clearly observed in $I_d - V_d$ plots in Fig. 4(a) at higher V_g as the pulsed width is not sufficiently small. At high V_g, we can clearly see the quasi-saturation behavior in $I_d - V_d$ characteristics as there is very little change in current with increase in V_g. The model for nonlinear access region resistance is able to capture this behavior accurately. Fig. 4(b) shows a sharp dip in g_{ds} which is the signature of self-heating effect. This sharp dip shows that g_{ds} changes sign and is negative for higher V_d values. Another important characteristic in HEMT is the reverse output characteristics shown in Fig. 4(c). The S-P based model can accurately capture the reverse output characteristics without any additional parameter or any extra parameter optimization effort, which is an advantage of a physics based model.

Now to extract the temperature dependence parameters, we have fitted measured $I_d - V_d$ and $I_d - V_g$ data at different temperatures (-20, 25, 50, 100, 150°C). For the used power HEMT device, extracted ON-resistance (sum of total source/drain and channel resistances) increases rapidly with the increase in temperature and is shown in Fig. 5. The model is able to predict this trend accurately. The simulation results with the experimental data validate our temperature dependent model of $R_{d/s}$ (which is the major component in R_{ON}) for a wide temperature range beyond just room temperature.

VI. Conclusion

A current dependent nonlinear source/drain access resistance model of AlGaN/GaN HEMTs devices is presented and verified with the TCAD and measured data for toshiba power GaN HEMT device. The carrier saturation velocity in the access region limits the maximum drain current supported through the device and is very important to accurately predict DC I-V characteristics at higher V_g. The temperature dependence of $R_{d/s}$ model is validated for a wide range of temperature. This model is implemented in the Verilog - A code of ASM-HEMT model within a physics based framework and has been tested for Agilent ADS, Synopsys HSPICE and Cadence's Spectre simulators.

Acknowledgment

This work was supported in part by DST Fast Track Scheme for Young Scientists, in part by ISRO, and in part by Ramanujan Fellowship. We would like to thank Toshiba

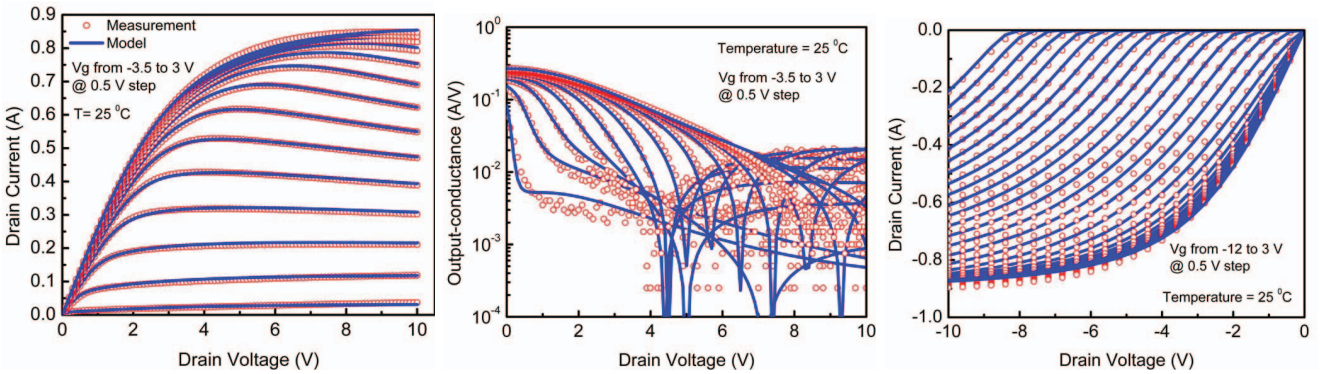

(a) (b) (c)

Fig. 4: (a) $I_d - V_d$, (b) output-conductance and (c) reverse output characteristics fitting with experimental data at room temperature (symbol: measurement, solid line: model); the non-linear access region resistance model shows correct behavior for the higher V_g curves in the $I_d - V_d$ plot; the S-P based model can accurately capture the reverse output characteristics.

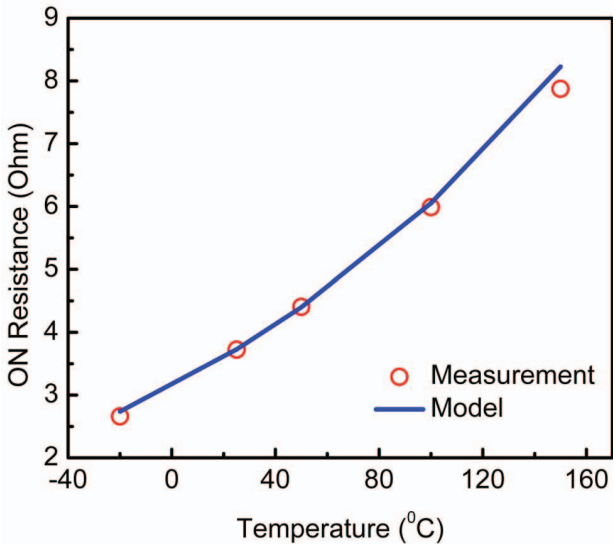

Fig. 5: The increase of R_{ON} with temperature for the power HEMT device. Model can correctly capture this variation of ON-resistance for a wide range of temperature.

Corporation for providing measurement data as a part of Si2-CMC model standardization activity.

REFERENCES

[1] R. Rupp, T. Laska, O. Haberlen, M. Treu, "Application specific trade-offs for WBG SiC, GaN and high end Si power switch technologies," *International Electron Devices Meeting (IEDM)*, Technical Digest. 15-17 Dec. 2014.

[2] U. K. Mishra, L. Shen, T. E. Kazior and Y. F. Wu, "GaN-Based RF Power Devices and Amplifiers," *Proceedings of the IEEE*, vol. 96, no. 2, pp. 287-305, Feb. 2008.

[3] Y.-F. Wu, D. Kapolnek, J.P. Ibbetson, P. Parikh, et. al., "Very-High Power Density AlGaN/GaN HEMTs," *IEEE Transactions on Electron Devices*, vol. 48, no. 3, pp. 586-590, 2001.

[4] K. Shinohara et al., "Scaling of GaN HEMTs and Schottky Diodes for Submillimeter-Wave MMIC Applications," *IEEE Transactions on Electron Devices*, vol. 60, no. 10, pp. 2982-2996, Oct. 2013.

[5] D.R. Greenberg, and J.A. del Alamo, "Velocity Saturation in the Extrinsic Device: A Fundamental Limit in HFETs," *IEEE Transactions on Electron Devices*, vol. 41, pp. 1334-39, August 1994.

[6] S. Khandelwal, "Compact Modeling solution for Advanced Semiconductor Devices", *PhD Thesis* 2013, Norwegian University of Sci. and Tech., ISSN 1503-8181; 2013:248.

[7] S. Khandelwal, Y.S. Chauhan, T.A Fjeldly, "Analytical Modeling of Surface-Potential and Intrinsic Charges in AlGaN/GaN HEMT Devices," *IEEE Transactions on Electron Devices*, vol.59, no.10, pp.2856-2860, Oct. 2012.

[8] S. Khandelwal, T.A. Fjeldly, "A physics based compact model of I-V and C-V characteristics in AlGaN/GaN HEMT devices," *Solid-State Electronics*, vol 76, October 2012, Pages 60-66, ISSN 0038-1101.

[9] S. Ghosh, A. Dasgupta, S. Khandelwal, S. Agnihotri and Y. S. Chauhan, "Surface-Potential-Based Compact Modeling of Gate Current in AlGaN/GaN HEMTs," *IEEE Transactions on Electron Devices*, vol. 62, no. 2, pp. 443-448, Feb. 2015.

[10] S. Ghosh, K. Sharma, S. Khandelwal, Y. S. Chauhan et. al., "Modeling of Temperature Effects in a Surface-Potential Based ASM-HEMT Model," *IEEE International Conference on Emerging Electronics (ICEE)*, Bangalore, India, 3-6 Dec. 2014.

[11] S. Khandelwal, S. Ghosh, Y. S. Chauhan, B. Iniguez and T. A. Fjeldly, "Surface-Potential-Based RF Large Signal Model for Gallium Nitride HEMTs," *IEEE Compound Semiconductor Integrated Circuit Symposium (CSICS)*, pp. 1-4, New Orleans, LA, 2015.

[12] S.D. Mertens, "Status of the GaN HEMT Standardization Effort at the Compact Model Coalition," *Compound Semiconductor Integrated Circuit Symposium (CSICs), 2014 IEEE*, pp.1,4, 19-22 Oct. 2014.

[13] S. Khandelwal, J. P. Duarte, A. Medury, Y. S. Chauhan, S. Salahuddin and C. Hu, "Modeling SiGe FinFETs With Thin Fin and Current-Dependent Source/Drain Resistance," *IEEE Electron Device Letters*, vol. 36, no. 7, pp. 636-638, July 2015.

[14] R. J. Trew, Yueying Liu, L. Bilbro, Weiwei Kuang, R. Vetury and J. B. Shealy, "Nonlinear source resistance in high-voltage microwave AlGaN/GaN HFETs," *IEEE Transactions on Microwave Theory and Techniques*, vol. 54, no. 5, pp. 2061-2067, May 2006.

[15] Y. Chengy, K. Imaiz, M-C. Jengx, Z. Liuk, et. al., "Modelling temperature effects of quarter micrometre MOSFETs in BSIM3v3 for circuit simulation," *Semicond. Sci. Technol*, vol. 12 pp. 1349-1354, 1997.

[16] Y. S. Chauhan, M. A. Karim, S. Venugopalan, H. Agarwal, et. al., " BSIM6.0 MOSFET Compact Model," *Technical Manual*, 2013.

[17] H. Morkoc, "carrier Transport," in *Nitride Semiconductor Devices: Fundamental and Applications,* Wiley-VCH, Verlag GmbH, Weinheim, 2013, ch. 4, sec. 3, pp. 147.

[18] W.S. Tan, M.J. Uren, P.W. Fry, P.A. Houston, et. al., "High temperature performance of AlGaN/GaN HEMTs on Si substrates," *Solid-State Electronics*, vol. 50, issue 3, Pages 511-513, March 2006.